

Information Gradient for Directed Acyclic Graphs: A Score-based Framework for End-to-End Mutual Information Maximization

Tadashi Wadayama

Nagoya Institute of Technology

wadayama@nitech.ac.jp

Abstract—This paper presents a general framework for end-to-end mutual information maximization in communication and sensing systems represented by stochastic directed acyclic graphs (DAGs). We derive a unified formula for the (mutual) information gradient with respect to arbitrary internal parameters, utilizing marginal and conditional score functions. We demonstrate that this gradient can be efficiently computed using vector-Jacobian products (VJP) within standard automatic differentiation frameworks, enabling the optimization of complex networks under global resource constraints. Numerical experiments on both linear multipath DAGs and nonlinear channels validate the proposed framework; the results confirm that the estimator, utilizing score functions learned via denoising score matching, accurately reproduces ground-truth gradients and successfully maximizes end-to-end mutual information. Beyond maximization, we extend our score-based framework to a novel unsupervised paradigm: digital twin calibration via Fisher divergence minimization.

Index Terms—mutual information, nonlinear Gaussian channels, score functions, denoising score matching, gradient-based optimization, directed acyclic graphs, information gradient

I. INTRODUCTION

Designing complex communication and sensing systems to maximize information flow is a central challenge in modern engineering. From next-generation wireless networks aiming for semantic communication [11] to distributed sensor fusion in IoT, the paradigm is shifting from optimizing individual modules to *end-to-end* system design. In these scenarios, mutual information (MI) [1] serves as the gold standard objective function, capturing nonlinear dependencies that simple correlations miss. However, maximizing MI in such high-dimensional, multi-stage systems presents a formidable computational barrier. Unlike deterministic loss functions (e.g., mean squared error) where gradients are easily computed via backpropagation, MI depends on the joint probability density, which evolves in complex ways through the system dynamics. Existing variational bounds focus primarily on *estimating* the MI value; utilizing them for gradient-based optimization of internal system parameters often leads to high variance and instability. Essentially, we lack a scalable mechanism to “backpropagate” information measures through complex stochastic graphs.

In a companion paper [2], we took a first step toward addressing this challenge by introducing the *information gradient* framework. This theory establishes an exact identity linking the gradient of MI to *score functions* [1], [10]—the gradients

of log-likelihoods. By leveraging modern score matching techniques [3]–[5], this framework allows for efficient gradient estimation without closed-form likelihoods. However, the scope of [2] was limited to single-stage channels of the form $Y = f_\eta(X) + Z$. Real-world systems are rarely this simple; they involve intricate topologies with branching paths, merging signals, and multi-hop processing, effectively forming stochastic networks. Applying the basic formula to such architectures is non-trivial, as a single parameter can influence the final output through multiple interacting pathways, complicating the derivation of the score function and the associated chain rules.

This paper generalizes the information gradient framework to arbitrary stochastic systems represented by *directed acyclic graphs (DAGs)*. We view the system as a computational graph where nodes represent stochastic variables and edges represent parameterized nonlinear transformations. This means that any stochastic network system implementable in modern automatic differentiation frameworks (e.g., PyTorch, TensorFlow, JAX) can now be optimized for MI using our score-based estimator.

Our main contribution is a unified gradient formula applicable to any internal parameter within a DAG, regardless of its depth or topological complexity. Crucially, we bridge the gap between information theory and deep learning implementation: we show that the generalized information gradient can be efficiently computed using standard *vector-Jacobian products (VJP)* [6]. Moreover, we demonstrate that canonical multi-user models, such as multiple access channels (MAC) and broadcast channels (BC), are naturally represented as DAGs. Consequently, our method serves as a unified numerical solver for exploring the achievable rate regions of complex nonlinear channels where closed-form analytical characterizations are intractable. To rigorously validate this capability, we show that our score-based information gradient exactly reproduces the known capacity region of the Gaussian MAC.

This generalization opens up broad practical applications. It enables the end-to-end optimization of transmitter and receiver neural networks over unknown nonlinear channels, a key requirement for *semantic communications*. Furthermore, we extend the framework to a novel unsupervised paradigm: *digital twin calibration*. By minimizing the Fisher divergence—a natural byproduct of our score-based formulation—we propose a method to align simulation parameters with physical reality using only output observations.

II. PRELIMINARIES

In this section, we introduce the basic notations and review key concepts regarding the fundamental information gradient identity established in our companion paper [2].

A. Notations

We use boldface lowercase letters (e.g., \mathbf{x}) to denote vectors and boldface uppercase letters (e.g., \mathbf{A}) for matrices. Random vectors are denoted by uppercase letters (e.g., X, Y), and their realizations by lowercase letters (e.g., \mathbf{x}, \mathbf{y}). The probability density function (PDF) of a continuous random vector X is denoted by $p_X(\mathbf{x})$. The expectation operator is denoted by $\mathbb{E}[\cdot]$. We use $h(X) \equiv -\mathbb{E}[\log p_X(X)]$ to denote the differential entropy of X , and $I(X; Y) \equiv h(Y) - h(Y|X)$ for the mutual information between X and Y [1]. The Jacobian matrix of a vector-valued differentiable function $\mathbf{f}(\mathbf{x})$ with respect to \mathbf{x} is denoted by $D_{\mathbf{x}}\mathbf{f} \equiv \frac{\partial \mathbf{f}}{\partial \mathbf{x}}$.

B. Score Functions

The gradient of the log-likelihood with respect to the data variable is termed the *score function* [1]. For a random vector $Y \in \mathbb{R}^d$ with PDF $p_Y(\mathbf{y})$, the (marginal) score function is defined as

$$\mathbf{s}_Y(\mathbf{y}) \equiv \nabla_{\mathbf{y}} \log p_Y(\mathbf{y}). \quad (1)$$

Similarly, the conditional score function for Y given X is $\mathbf{s}_{Y|X}(\mathbf{y}|x) \equiv \nabla_{\mathbf{y}} \log p_{Y|X}(\mathbf{y}|x)$. A fundamental property of the score function is that its expectation under the corresponding distribution is zero, provided that the PDF vanishes at the boundary:

$$\begin{aligned} \mathbb{E}[\mathbf{s}_Y(Y)] &= \int p_Y(\mathbf{y}) \nabla_{\mathbf{y}} \log p_Y(\mathbf{y}) d\mathbf{y} \\ &= \int \nabla_{\mathbf{y}} p_Y(\mathbf{y}) d\mathbf{y} = \mathbf{0}. \end{aligned} \quad (2)$$

This property plays a crucial role in simplifying gradient derivations.

C. Related works

Our framework including [9] is grounded in the deep correspondence between information theory and thermodynamics, specifically the interpretation of noise injection as a diffusion process. This perspective originates from Stam [14], who utilized the de Bruijn identity—relating the derivative of entropy to Fisher information—to establish the entropy power inequality. Building on this diffusion-based view, Brown [15] and Barron [16] developed the entropic central limit theorem, proving the monotonic convergence of Fisher information. In the context of Gaussian channels, Guo, Shamai, and Verdú [17] unified these concepts through the I-MMSE relationship, identifying the derivative of mutual information with the minimum mean-square error.

While these classical studies primarily employed these relationships for theoretical proofs of inequalities, our work repurposes them for practical computation. We extend the utility of these fundamental identities from theoretical analysis to data-driven optimization. By generalizing these connections

to arbitrary stochastic DAGs and estimating the requisite score functions from data, we transform these classical thermodynamic links into a scalable engine for end-to-end mutual information maximization.

D. Information Gradient Identity

In our companion paper [2], we derived a fundamental identity that relates the gradient of mutual information to score functions. Consider a general parameterized system where the output is given by $Y = f_{\eta}(X) + Z$, with input $X \in \mathbb{R}^n$, where $f_{\eta} : \mathbb{R}^n \rightarrow \mathbb{R}^m$ is a differentiable function parameterized by $\eta \in \mathbb{R}^d$, and $Z \in \mathbb{R}^m$ is an additive noise vector. Under standard regularity conditions, the gradient of the mutual information with respect to η can be expressed as

$$\nabla_{\eta} I(X; Y) = \mathbb{E} [(D_{\eta} Y)^{\top} (\mathbf{s}_{Y|X}(Y|X) - \mathbf{s}_Y(Y))]. \quad (3)$$

This identity states that the information gradient is the expected inner product of the Jacobian of the output with respect to the parameters, and a “score difference” vector. While the paper [2] focuses on the theoretical derivation and properties of this identity for basic channel models, the present paper generalizes this formula for complex stochastic networks represented by general DAGs.

E. Denoising Score Matching

Since the true data distributions are typically unknown in complex systems, we must estimate the score functions from data. Denoising score matching (DSM) [3]–[5] is a highly effective technique for this purpose. When the data \mathbf{y} is generated by adding Gaussian noise $\mathbf{z} \sim \mathcal{N}(\mathbf{0}, \sigma^2 \mathbf{I})$ to a clean sample $\tilde{\mathbf{y}}$, i.e., $\mathbf{y} = \tilde{\mathbf{y}} + \mathbf{z}$, a score model $\mathbf{s}_{\phi}(\mathbf{y})$ parameterized by a parameter vector ϕ can be trained by minimizing the following objective:

$$\mathcal{J}_{\text{DSM}}(\phi) = \mathbb{E}_{\tilde{\mathbf{y}}, \mathbf{z}} \left[\left\| \mathbf{s}_{\phi}(\tilde{\mathbf{y}} + \mathbf{z}) + \frac{\mathbf{z}}{\sigma^2} \right\|^2 \right]. \quad (4)$$

Minimizing this objective ensures that $\mathbf{s}_{\phi}(\mathbf{y})$ approximates the true score $\nabla_{\mathbf{y}} \log p_Y(\mathbf{y})$. We utilize this technique to learn the necessary score functions for gradient estimation.

While DSM are mainly used throughout this paper, it should be noted that the velocity field framework (e.g., flow matching [18] and rectified flow [19]) could be employed to derive a score function in a data-driven manner. Since there exists a one-to-one algebraic correspondence between the score function and the velocity field, we can derive a score function from a velocity field. In practice, training a velocity field might be significantly more stable than its score-based counterpart, especially in low-noise regimes. In such cases, the use of the velocity field framework for score function estimation might be more advantageous.

III. INFORMATION GRADIENT FOR CASCADED CHANNELS

It is beneficial to consider the cascade case as a building block for more complex systems represented by DAGs. In this section, we derive the information gradient for a cascade of deterministic functions with additive Gaussian noises.

A. Problem setup

Without loss of generality, we consider an N -stage cascaded nonlinear Gaussian channels. Let $X \in \mathbb{R}^{d_0}$ be the random input source vector following a prior probability density function (PDF) p_X . The cascaded channel consists of a sequence of N computational blocks, where the output of the i -th block, denoted by $Y_i \in \mathbb{R}^{d_i}$, serves as the input to the $(i+1)$ -th block.

We assume that each block $i \in \{1, \dots, N\}$ consists of a parameterized deterministic mapping followed by an additive Gaussian noise channel. Specifically, the relationship between consecutive intermediate variables is given by

$$Y_i = f_{\eta_i}(Y_{i-1}) + Z_i, \quad i = 1, \dots, N, \quad (5)$$

where $Y_0 \triangleq X$ is the system input, and $Y \equiv Y_N$ represents the final output of the cascaded channel. Here, $f_{\eta_i} : \mathbb{R}^{d_{i-1}} \rightarrow \mathbb{R}^{d_i}$ is a deterministic differentiable function parameterized by a parameter vector η_i . The noise vector $Z_i \in \mathbb{R}^{d_i}$ is assumed to be independent and identically distributed (i.i.d.) Gaussian random variables with zero mean and covariance matrix $\sigma_i^2 \mathbf{I}$ ($\sigma_i > 0$), which are independent of X and $\{Z_j\}_{j \neq i}$. Figure 1 shows a schematic representation of the cascaded channel.

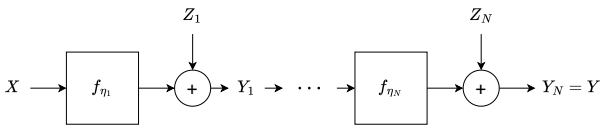


Fig. 1. A schematic representation of an N -stage cascaded nonlinear Gaussian channel. Each stage i consists of a deterministic mapping f_{η_i} followed by additive Gaussian noise Z_i . The system forms a Markov chain $X \rightarrow Y_1 \rightarrow \dots \rightarrow Y_N = Y$.

Due to the noise injection at each stage, the mapping from X to any intermediate output Y_i (including the final output $Y = Y_N$) is stochastic. The entire cascade forms a Markov chain:

$$X \rightarrow Y_1 \rightarrow Y_2 \rightarrow \dots \rightarrow Y_N = Y. \quad (6)$$

We assume that P_Y and $P_{Y|X}$ exist and are differentiable.

Our primary goal is to maximize the end-to-end MI between the initial input X and the final output Y by optimizing the set of parameters $\{\eta_1, \dots, \eta_N\}$. The optimization problem is defined by

$$\text{maximize}_{\{\eta_i\}} \quad I(X; Y). \quad (7)$$

To employ gradient-based optimization methods, we need to compute the gradient of this objective with respect to any intermediate parameter η_k ($1 \leq k \leq N$), i.e., $\nabla_{\eta_k} I(X; Y)$.

B. Derivation of the Gradient Formula

We now derive the gradient of the mutual information $I(X; Y)$ with respect to a parameter vector η_k in the k -th block. By the definition of mutual information, we have

$$I(X; Y) = h(Y) - h(Y|X), \quad (8)$$

where $h(\cdot)$ denotes the differential entropy. The gradient can therefore be decomposed into two terms:

$$\nabla_{\eta_k} I(X; Y) = \nabla_{\eta_k} h(Y) - \nabla_{\eta_k} h(Y|X). \quad (9)$$

First, let us consider the gradient of the marginal entropy $h(Y) = -\mathbb{E}[\log p_Y(Y)]$. It is important to note that the final output Y is a random variable whose value depends on the parameter η_k through the deterministic mappings in the cascade. We can view Y as a differentiable function of the input X , all noise variables $\{Z_i\}_{i=1}^N$, and the parameters $\{\eta_i\}_{i=1}^N$. Applying the chain rule to the expectation (assuming standard regularity conditions that allow interchanging differentiation and expectation), we obtain:

$$\begin{aligned} \nabla_{\eta_k} h(Y) &= -\mathbb{E}[\nabla_{\eta_k} \log p_Y(Y)] \\ &= -\mathbb{E}\left[(D_{\eta_k} Y)^\top \nabla_{\mathbf{y}} \log p_Y(\mathbf{y}) \Big|_{\mathbf{y}=Y}\right] \\ &\quad - \mathbb{E}\left[\frac{\partial}{\partial \eta_k} \log p_Y(\mathbf{y}; \eta_k) \Big|_{\mathbf{y}=Y}\right], \end{aligned} \quad (10)$$

where $D_{\eta_k} Y \equiv \frac{\partial Y}{\partial \eta_k}$ is the Jacobian matrix of Y with respect to η_k . The second term on the right-hand side vanishes because

$$\mathbb{E}_Y [\nabla_{\eta_k} \log p_Y(Y; \eta_k)] = \int \nabla_{\eta_k} p_Y(\mathbf{y}; \eta_k) d\mathbf{y} \quad (11)$$

$$= \nabla_{\eta_k} \int p_Y(\mathbf{y}) d\mathbf{y} \quad (12)$$

$$= \nabla_{\eta_k} 1 = 0. \quad (13)$$

This equation reflects the well-known property that the expectation of the score function of the marginal distribution is zero. By introducing the *marginal score function* $s_Y(\mathbf{y}) \equiv \nabla_{\mathbf{y}} \log p_Y(\mathbf{y})$, we have

$$\nabla_{\eta_k} h(Y) = -\mathbb{E}[(D_{\eta_k} Y)^\top s_Y(Y)]. \quad (14)$$

Similarly, for the conditional entropy

$$h(Y|X) = -\mathbb{E}[\log p_{Y|X}(Y|X)], \quad (15)$$

we can derive its gradient by conditioning on X . Let

$$s_{Y|X}(\mathbf{y}|\mathbf{x}) \equiv \nabla_{\mathbf{y}} \log p_{Y|X}(\mathbf{y}|\mathbf{x}) \quad (16)$$

be the *conditional score function*. Following the same logic as above, we obtain:

$$\nabla_{\eta_k} h(Y|X) = -\mathbb{E}[(D_{\eta_k} Y)^\top s_{Y|X}(Y|X)]. \quad (17)$$

Substituting (14) and (17) into (9) yields the following key result.

Theorem 1 (Information Gradient for Cascaded Channels). *The gradient of the end-to-end mutual information $I(X; Y)$ with respect to the parameter η_k of the k -th ($k \in \{1, \dots, N\}$) block is given by*

$$\nabla_{\eta_k} I(X; Y) = \mathbb{E}[(D_{\eta_k} Y)^\top (s_{Y|X}(Y|X) - s_Y(Y))]. \quad (18)$$

This formula has an intuitive interpretation: the gradient is the expected product of the Jacobian $D_{\eta_k} Y$, which represents how the parameter η_k affects the final output, and a

“score difference” term ($s_{Y_N|X} - s_{Y_N}$), which represents the information-theoretic learning signal.

Remark 1 (Posterior Score Representation). A crucial observation is that the score difference term can be equivalently expressed using the posterior distribution:

$$s_{Y|X}(\mathbf{y}|\mathbf{x}) - s_Y(\mathbf{y}) = \nabla_{\mathbf{y}} \log p_{X|Y}(\mathbf{x}|\mathbf{y}). \quad (19)$$

This identity follows readily from Bayes’ rule, $\log p(\mathbf{y}|\mathbf{x}) - \log p(\mathbf{y}) = \log p(\mathbf{x}|\mathbf{y}) - \log p(\mathbf{x})$, by taking the gradient with respect to \mathbf{y} (noting that $\nabla_{\mathbf{y}} \log p(\mathbf{x}) = 0$). Consequently, the information gradient can be re-expressed as

$$\nabla_{\boldsymbol{\eta}_k} I(X; Y) = \mathbb{E} \left[(D_{\boldsymbol{\eta}_k} Y)^\top \nabla_{\mathbf{y}} \log p_{X|Y}(X|\mathbf{y}) \Big|_{\mathbf{y}=\mathbf{Y}} \right]. \quad (20)$$

This “posterior score” form is particularly useful for implementations that utilize an approximate inference model.

Remark 2 (Reduction to Single-Stage Gradient). It is illuminating to consider the simplest case, a single-stage channel ($N = 1$), given by $Y_1 = f_{\boldsymbol{\eta}_1}(X) + Z_1$. In this case, the conditional entropy $h(Y_1|X) = h(Z_1)$ is constant with respect to $\boldsymbol{\eta}_1$, implying $\nabla_{\boldsymbol{\eta}_1} h(Y_1|X) = 0$. Consequently, the conditional score term in (18) vanishes in expectation

$$\mathbb{E}[(D_{\boldsymbol{\eta}_1} Y_1)^\top s_{Y_1|X}(Y_1|X)] = 0. \quad (21)$$

Theorem 1 then reduces to

$$\nabla_{\boldsymbol{\eta}_1} I(X; Y_1) = -\mathbb{E} \left[(D_{\boldsymbol{\eta}_1} Y_1)^\top s_{Y_1}(Y_1) \right], \quad (22)$$

which perfectly recovers the information gradient formula for standard nonlinear Gaussian channels derived in [2]. Our generalized theorem reveals that for deeper cascades ($N > 1$), the additional term $s_{Y_N|X}$ becomes necessary because intermediate noise injections make $h(Y_N|X)$ dependent on earlier parameters.

C. Efficient Gradient Computation

The formula derived in Theorem 1 involves the Jacobian matrix $D_{\boldsymbol{\eta}_k} Y$, which can be computationally expensive if explicitly instantiated, especially for high-dimensional systems. However, by exploiting the cascade structure and modern automatic differentiation (AD) techniques, we can compute this gradient efficiently without ever forming the full Jacobian matrix.

1) Chain Rule for Cascaded Jacobian: Due to the Markovian structure of the cascade, the Jacobian $D_{\boldsymbol{\eta}_k} Y$ can be decomposed using the chain rule. Recall that Y_N depends on $\boldsymbol{\eta}_k$ only through the intermediate sequence $Y_k, Y_{k+1}, \dots, Y_{N-1}$. The Jacobian can be explicitly written as a product of Jacobians of purely deterministic mappings:

$$D_{\boldsymbol{\eta}_k} Y = \left(\prod_{i=N}^{k+1} \frac{\partial f_{\boldsymbol{\eta}_i}}{\partial Y_{i-1}}(Y_{i-1}) \right) \cdot \frac{\partial f_{\boldsymbol{\eta}_k}}{\partial \boldsymbol{\eta}_k}(Y_{k-1}). \quad (23)$$

Here, $\frac{\partial f_{\boldsymbol{\eta}_i}}{\partial Y_{i-1}}$ is the Jacobian of the i -th block’s function with respect to its input, and $\frac{\partial f_{\boldsymbol{\eta}_k}}{\partial \boldsymbol{\eta}_k}$ is the Jacobian with respect to its parameter. This product structure perfectly matches the

backward pass of standard backpropagation algorithms used in training deep neural networks.

2) Vector-Jacobian Product (VJP): More importantly, the gradient formula (18) does not require the full Jacobian matrix itself, but rather its transpose multiplied by a vector. Let us define the *information score vector* $\mathbf{v} \in \mathbb{R}^{d_N}$ as

$$\mathbf{v}(\mathbf{x}, \mathbf{y}) \equiv s_{Y|X}(\mathbf{y}|\mathbf{x}) - s_Y(\mathbf{y}). \quad (24)$$

The gradient term inside the expectation is then $(D_{\boldsymbol{\eta}_k} Y)^\top \mathbf{v}$. This operation is known as a vector-Jacobian product (VJP) [6]. In standard AD frameworks (like PyTorch, TensorFlow, or JAX), VJP can be computed efficiently in a single backward pass by treating \mathbf{v} as the initial gradient (or “adjoint”) at the output layer.

In practice, the VJP can be effortlessly computed by defining a scalar surrogate loss function. Let $\text{stop}(\cdot)$ denote the stop-gradient operator, which acts as the identity function during the forward pass but has zero gradient during the backward pass in the AD framework. We define the VJP loss as

$$\mathcal{L}_{\text{VJP}}(\boldsymbol{\eta}) \equiv -\langle \text{stop}(\mathbf{v}), Y \rangle, \quad (25)$$

where $\langle \cdot, \cdot \rangle$ denotes the inner product. Applying standard automatic differentiation to this loss yields

$$\nabla_{\boldsymbol{\eta}_k} \mathcal{L}_{\text{VJP}} = -(D_{\boldsymbol{\eta}_k} Y)^\top \mathbf{v}. \quad (26)$$

The expectation of this term exactly recovers the negative of the information gradient derived in (18). In practical implementations, we can obtain a Monte Carlo estimator of the true information gradient by taking the sample mean of $\nabla_{\boldsymbol{\eta}_k} \mathcal{L}_{\text{VJP}}$ over a mini-batch. For a mini-batch of B samples $\{(\mathbf{x}^{(b)}, \mathbf{y}^{(b)})\}_{b=1}^B$, a Monte Carlo estimator of the information gradient is given by

$$\widehat{\nabla_{\boldsymbol{\eta}_k} I} = -\frac{1}{B} \sum_{b=1}^B \nabla_{\boldsymbol{\eta}_k} \mathcal{L}_{\text{VJP}}(\boldsymbol{\eta}_k; \mathbf{x}^{(b)}, \mathbf{y}^{(b)}). \quad (27)$$

This estimator allows for maximizing mutual information via standard stochastic gradient descent (SGD).

D. Score Model Approximation

The information gradient formula (18) relies on the true marginal score $s_Y(\mathbf{y})$ and conditional score $s_{Y|X}(\mathbf{y}|\mathbf{x})$, which are generally unknown for complex nonlinear cascades. To make the proposed framework practical, we employ parameterized score models, typically deep neural networks, to approximate these functions.

Let $s_{\phi}(\mathbf{y}; \boldsymbol{\eta})$ and $s_{\psi}(\mathbf{y}|\mathbf{x}; \boldsymbol{\eta})$ be the score models parameterized by ϕ and ψ , respectively, designed to approximate the true scores:

$$s_{\phi}(\mathbf{y}; \boldsymbol{\eta}) \approx \nabla_{\mathbf{y}} \log p_Y(\mathbf{y}; \boldsymbol{\eta}), \quad (28)$$

$$s_{\psi}(\mathbf{y}|\mathbf{x}; \boldsymbol{\eta}) \approx \nabla_{\mathbf{y}} \log p_{Y|X}(\mathbf{y}|\mathbf{x}; \boldsymbol{\eta}). \quad (29)$$

Note that these models implicitly depend on the cascade parameters $\boldsymbol{\eta} = \{\boldsymbol{\eta}_i\}_{i=1}^N$ since the distributions of Y change with $\boldsymbol{\eta}$. Crucially, these score models can be efficiently trained

from samples using DSM [3]–[5] or its variants, without requiring knowledge of the underlying likelihoods. For standard Gaussian noise channels at the final stage, DSM provides a simple and tractable objective.

Replacing the true scores with their learned counterparts yields a practical surrogate VJP loss for a sample (\mathbf{x}, \mathbf{y}) :

$$\mathcal{L}_{\text{VJP}}(\boldsymbol{\eta}_k; \mathbf{x}, \mathbf{y}) \equiv -\langle \text{stop}(s_{\psi}(\mathbf{y}|\mathbf{x}) - s_{\phi}(\mathbf{y})), \mathbf{y} \rangle. \quad (30)$$

Optimizing the cascade parameters $\boldsymbol{\eta}$ using gradients derived from this surrogate loss, while simultaneously (or alternately) training the score models ϕ, ψ to track the changing distributions, constitutes the core of our proposed end-to-end optimization framework.

E. Analytical Example: Linear Gaussian Cascaded Channel

To validate the proposed information gradient formula (Theorem 1), we consider a simple two-stage linear Gaussian cascade where the exact gradient is analytically tractable. Let the input be $X \sim \mathcal{N}(0, \sigma_X^2)$. Consider a two-stage cascade ($N = 2$) with scalar variables:

$$Y_1 = \eta_1 X + Z_1, \quad Z_1 \sim \mathcal{N}(0, \sigma_1^2), \quad (31)$$

$$Y_2 = Y_1 + Z_2, \quad Z_2 \sim \mathcal{N}(0, \sigma_2^2), \quad (32)$$

where η_1 is the scalar parameter of interest in the first stage. The total effective noise is $Z_{\text{eff}} = Z_1 + Z_2 \sim \mathcal{N}(0, \sigma_N^2)$ with $\sigma_N^2 = \sigma_1^2 + \sigma_2^2$. The final output is $Y_2 = \eta_1 X + Z_{\text{eff}}$, with variance $v_{Y_2} \equiv \text{Var}(Y_2) = \eta_1^2 \sigma_X^2 + \sigma_N^2$.

The mutual information for this scalar Gaussian channel is known to be

$$I(X; Y_2) = \frac{1}{2} \log \left(1 + \frac{\eta_1^2 \sigma_X^2}{\sigma_N^2} \right) = \frac{1}{2} \log \left(\frac{v_{Y_2}}{\sigma_N^2} \right). \quad (33)$$

Differentiating this directly with respect to η_1 yields the true gradient:

$$\frac{\partial I(X; Y_2)}{\partial \eta_1} = \frac{1}{2} \frac{\sigma_N^2}{v_{Y_2}} \cdot \frac{2\eta_1 \sigma_X^2}{\sigma_N^2} = \frac{\eta_1 \sigma_X^2}{v_{Y_2}}. \quad (34)$$

Now we apply Theorem 1. The Jacobian of the final output Y_2 with respect to η_1 is $D_{\eta_1} Y_2 = \frac{\partial}{\partial \eta_1} (\eta_1 X + Z_1 + Z_2) = X$. The marginal score is $s_{Y_2}(y) = -y/v_{Y_2}$, and the conditional score is $s_{Y_2|X}(y|x) = -(y - \eta_1 x)/\sigma_N^2$. Substituting these into (18):

$$\begin{aligned} \nabla_{\eta_1} I &= \mathbb{E} \left[X \cdot \left(-\frac{Y_2 - \eta_1 X}{\sigma_N^2} - \left(-\frac{Y_2}{v_{Y_2}} \right) \right) \right] \\ &= -\frac{\mathbb{E}[XY_2] - \eta_1 \mathbb{E}[X^2]}{\sigma_N^2} + \frac{\mathbb{E}[XY_2]}{v_{Y_2}}. \end{aligned} \quad (35)$$

Using $\mathbb{E}[X^2] = \sigma_X^2$ and $\mathbb{E}[XY_2] = \mathbb{E}[X(\eta_1 X + Z_{\text{eff}})] = \eta_1 \sigma_X^2$, the first term vanishes:

$$-\frac{\eta_1 \sigma_X^2 - \eta_1 \sigma_X^2}{\sigma_N^2} + \frac{\eta_1 \sigma_X^2}{v_{Y_2}} = \frac{\eta_1 \sigma_X^2}{v_{Y_2}}. \quad (36)$$

This exactly matches the classical result in (34), confirming the validity of our generalized information gradient formula.

IV. GENERALIZATION TO DIRECTED ACYCLIC GRAPHS

Having established the information gradient for cascaded channels, we now extend our framework to general stochastic networks represented by directed acyclic graphs (DAGs). This generalization allows us to optimize complex systems involving branching, merging, and parallel processing paths.

A. Problem Setup

Consider a communication or sensing system represented by a directed acyclic graph (DAG) $\mathcal{G} = (\mathcal{V}, \mathcal{E})$ with M nodes. Let V_1, \dots, V_M denote the random vectors associated with the nodes in a topological order. The network input is represented by a subset of root nodes, collectively denoted by X . Each subsequent node V_j is computed from its parent nodes $\text{Pa}(V_j)$ via a parameterized deterministic mapping, optionally corrupted by independent additive noise. Specifically, the local computation at node V_j is given by

$$V_j = f_j(\text{Pa}(V_j); \boldsymbol{\eta}_j) + Z_j, \quad (37)$$

where $f_j : \mathbb{R}^{d_j^{\text{in}}} \rightarrow \mathbb{R}^{d_j^{\text{out}}}$ is a differentiable function parameterized by $\boldsymbol{\eta}_j$, and Z_j is a zero-mean independent Gaussian noise vector (if node V_j is deterministic, $Z_j \equiv 0$). The set of all network parameters is $\boldsymbol{\eta} \equiv \{\boldsymbol{\eta}_j\}_j$, and the set of all noise sources is $\mathcal{Z} \equiv \{Z_j\}_j$.

The final output of the system, denoted by Y , is a subset of the leaf nodes. Thanks to the acyclic structure of \mathcal{G} , recursively substituting the parent nodes in (37) is guaranteed to terminate. Consequently, the end-to-end relationship from the roots X to the outputs Y can be explicitly expressed as a deterministic composition of the input X and all involved noise sources \mathcal{Z} :

$$Y = g(X, \mathcal{Z}; \boldsymbol{\eta}). \quad (38)$$

Figure 2 shows a schematic representation of a DAG network. To ensure the existence of the necessary score functions, we assume sufficient noise is injected into the network (typically at the final output nodes) such that Y admits a differentiable probability density function.

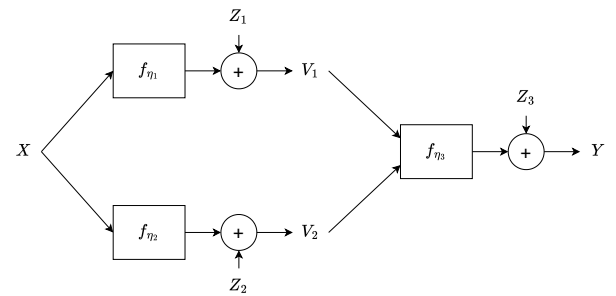


Fig. 2. An illustrative DAG network. The input X branches into two parallel paths, each processed by a distinct function f_{η_i} and corrupted by noise Z_i to produce intermediate nodes V_1, V_2 . These are then merged by function f_{η_3} and further corrupted by noise Z_3 to yield the final output Y .

B. Information Gradient Formula for DAG channels

We now derive the gradient of the mutual information $I(X; Y)$ with respect to an arbitrary parameter vector $\eta_k \in \eta$ within the DAG. Remarkably, the gradient formula retains the same elegant structure as in the cascade case, demonstrating its universality.

Theorem 2 (Information Gradient for DAGs). *Under standard regularity conditions, the gradient of the end-to-end mutual information $I(X; Y)$ with respect to any internal parameter η_k in a DAG is given by*

$$\nabla_{\eta_k} I(X; Y) = \mathbb{E} [(D_{\eta_k} Y)^\top (s_{Y|X}(Y|X) - s_Y(Y))], \quad (39)$$

where $D_{\eta_k} Y \equiv \frac{\partial g(X, \mathcal{Z}; \eta)}{\partial \eta_k}$ is the Jacobian of the final output with respect to η_k , and the expectation is taken over all random variables (X, \mathcal{Z}) in the network.

Proof: The mutual information is $I(X; Y) = h(Y) - h(Y|X)$. We analyze the gradient of the marginal entropy $h(Y) = -\mathbb{E}[\log p_Y(Y)]$ first. Unlike the cascade case, the expectation is now taken over the joint distribution of all inputs and noise sources in the DAG. Let $\omega = (X, \mathcal{Z})$ denote the collection of all primitive random variables in the network. The output Y is a deterministic function $Y = g(\omega; \eta)$. Assuming regularity conditions that permit interchanging ∇_{η_k} and \mathbb{E}_ω , we have:

$$\nabla_{\eta_k} h(Y) = -\mathbb{E}_\omega [\nabla_{\eta_k} \log p_Y(g(\omega; \eta); \eta)] \quad (40)$$

$$= -\mathbb{E}_\omega \left[(D_{\eta_k} Y)^\top \nabla_y \log p_Y(y) \Big|_{y=Y} \right] \\ - \mathbb{E}_\omega \left[\frac{\partial}{\partial \eta_k} \log p_Y(y; \eta) \Big|_{y=Y} \right]. \quad (41)$$

The second term is $\mathbb{E}_Y [\nabla_{\eta_k} \log p_Y(Y; \eta)]$, which vanishes due to the score function property $\int \nabla p = \nabla \int p = 0$. Thus, $\nabla_{\eta_k} h(Y) = -\mathbb{E} [(D_{\eta_k} Y)^\top s_Y(Y)]$. Following a strictly analogous argument for the conditional entropy term (conditioning on X throughout), we obtain $\nabla_{\eta_k} h(Y|X) = -\mathbb{E} [(D_{\eta_k} Y)^\top s_{Y|X}(Y|X)]$. Combining these results yields the claim of the theorem. ■

Crucially, the Jacobian $D_{\eta_k} Y$ in a DAG can be efficiently computed using standard reverse-mode automatic differentiation (backpropagation) through the graph, exactly as in modern deep learning frameworks. This means the VJP-based efficient computation strategy described in Section III-C applies directly to general DAGs without modification.

Remark 3 (Mathematical Importance of Acyclicity). The assumption that the graph \mathcal{G} is acyclic (DAG) is fundamental to our framework for two key reasons:

- 1) **Well-defined Composition:** The absence of cycles guarantees that the recursive computation terminates in finite steps. This ensures that the end-to-end mapping $Y = g(X, \mathcal{Z}; \eta)$ is a strictly well-defined composite function. If cycles were present, the system would be self-referential, requiring fixed-point formulations.
- 2) **Applicability of Chain Rule:** Because Y is a standard composite function, its Jacobian $D_{\eta_k} Y$ is rigorously

guaranteed to exist (under local differentiability assumptions) and can be computed via the standard multivariate chain rule. This theoretical guarantee legitimizes the use of backpropagation (VJP) for efficient computation.

Remark 4 (Reparameterization and Differentiability). A natural question arises regarding the differentiability of the stochastic output Y with respect to parameters η . Our framework relies on the *reparameterization trick* [20] (also known as the pathwise derivative estimator). As explicitly formulated in (38), we treat the system output not as a mere random variable, but as a deterministic function $Y = g(X, \mathcal{Z}; \eta)$ of the parameters and fixed independent noise sources \mathcal{Z} . Since the randomness is externalized into \mathcal{Z} which does not depend on η , the Jacobian $D_\eta Y$ is well-defined for any fixed realization of (X, \mathcal{Z}) . This perspective effectively decouples the randomness from the parametric dependence, allowing the gradient to “flow” through the stochastic nodes via standard backpropagation.

Remark 5 (Generality of Noise Assumptions). While this paper primarily assumes Gaussian noise for efficient score matching (DSM), the derived information gradient formulas theoretically hold for any noise distribution that admits a differentiable probability density function. Furthermore, noise injection is not required at every node. As long as sufficient noise enters the DAG (typically at the final output or accumulated along the path) to ensure the output Y admits a smooth density, intermediate transformations can be purely deterministic ($Z_j \equiv 0$). This flexibility allows our framework to model systems with mixed stochastic and deterministic components, such as digital logic combined with analog transmission.

C. Analytical Example: Multipath DAG

To further validate the generalized information gradient for DAGs (Theorem 2), we consider a multipath network where parameters affect the output through different topological structures. Consider the DAG shown in Fig. 2 with the following linear Gaussian specifications:

$$V_1 = \eta_1 X + Z_1, \quad Z_1 \sim \mathcal{N}(0, \sigma_1^2) \quad (42)$$

$$V_2 = X + Z_2, \quad Z_2 \sim \mathcal{N}(0, \sigma_2^2) \quad (43)$$

$$Y = \eta_2 V_1 + V_2 + Z_3, \quad Z_3 \sim \mathcal{N}(0, \sigma_3^2) \quad (44)$$

where $X \sim \mathcal{N}(0, \sigma_X^2)$. Here, η_1 is a deep parameter affecting only one path, while η_2 is a mixing parameter at the merge node. Crucially, η_2 affects both the signal gain and the effective noise variance. The end-to-end relationship is $Y = G_{\text{eff}} X + Z_{\text{eff}}$, where $G_{\text{eff}} = \eta_1 \eta_2 + 1$ is the effective gain and $Z_{\text{eff}} = \eta_2 Z_1 + Z_2 + Z_3$ is the effective noise with variance $\sigma_N^2 = \eta_2^2 \sigma_1^2 + \sigma_2^2 + \sigma_3^2$. The output variance is $\sigma_Y^2 = G_{\text{eff}}^2 \sigma_X^2 + \sigma_N^2$.

The mutual information is simply given by $I(X; Y) = \frac{1}{2} \log(\sigma_Y^2 / \sigma_N^2)$. Direct differentiation yields the true analytical

gradients:

$$\frac{\partial I}{\partial \eta_1} = \frac{\eta_2 G_{\text{eff}} \sigma_X^2}{v_Y} \quad (45)$$

$$\frac{\partial I}{\partial \eta_2} = \frac{\eta_1 G_{\text{eff}} \sigma_X^2 + \eta_2 \sigma_1^2}{v_Y} - \frac{\eta_2 \sigma_1^2}{\sigma_N^2} \quad (46)$$

We now apply Theorem 2. The Jacobians $D_{\eta_k} Y$ are derived via the chain rule over the DAG:

$$D_{\eta_1} Y = \eta_2 X, \quad D_{\eta_2} Y = V_1 = \eta_1 X + Z_1. \quad (47)$$

Using the Gaussian scores $s_Y(y) = -y/v_Y$ and $s_{Y|X}(y|x) = -(y - G_{\text{eff}}x)/\sigma_N^2 = -Z_{\text{eff}}/\sigma_N^2$, we verify the theorem: For η_1 , since $\mathbb{E}[XZ_{\text{eff}}] = 0$:

$$\nabla_{\eta_1} I = \mathbb{E} [\eta_2 X (s_{Y|X} - s_Y)] = \eta_2 \mathbb{E} \left[X \frac{Y}{v_Y} \right] = \frac{\eta_2 G_{\text{eff}} \sigma_X^2}{v_Y}. \quad (48)$$

This exactly matches (45). For η_2 , the Jacobian V_1 is correlated with Z_{eff} via Z_1 :

$$\begin{aligned} \nabla_{\eta_2} I &= \mathbb{E} \left[V_1 \left(-\frac{Z_{\text{eff}}}{\sigma_N^2} + \frac{Y}{v_Y} \right) \right] \\ &= -\frac{\mathbb{E}[(\eta_1 X + Z_1)(\eta_2 Z_1 + \dots)]}{\sigma_N^2} + \frac{\mathbb{E}[V_1 Y]}{v_Y} \\ &= -\frac{\eta_2 \sigma_1^2}{\sigma_N^2} + \frac{\eta_1 G_{\text{eff}} \sigma_X^2 + \eta_2 \sigma_1^2}{v_Y}. \end{aligned} \quad (49)$$

This perfectly recovers (46). This confirms that our framework correctly handles complex dependencies where parameters simultaneously affect signal paths and noise characteristics.

D. Algorithm for Information Gradient Estimation

The information gradient formula (39) allows us to estimate the information gradient for any parameter in the DAG using a Monte Carlo approach. Algorithm 1 outlines the procedure to obtain a mini-batch estimate of the gradient $\nabla_{\eta_k} I(X; Y)$ for a target parameter η_k . We assume that the necessary score models $s_{\phi}(\mathbf{y}) \approx \nabla_{\mathbf{y}} \log p_{\mathbf{Y}}(\mathbf{y})$ and $s_{\psi}(\mathbf{y}|\mathbf{x}) \approx \nabla_{\mathbf{y}} \log p_{\mathbf{Y}|X}(\mathbf{y}|\mathbf{x})$ have been pre-trained or are being trained concurrently.

This estimation procedure efficiently computes the gradients for *all* parameters in the DAG simultaneously in a single backward pass, not just for one specific η_k .

E. Integral Representation of Mutual Information

1) *Path Integral Representation*: While our primary focus is gradient-based optimization, the proposed framework also enables the estimation of the mutual information value $I(X; Y)$ itself. By leveraging the fundamental theorem of line integrals, we can reconstruct the mutual information from its gradients:

$$I(X; Y; \boldsymbol{\eta}) = I(X; Y; \boldsymbol{\eta}_0) + \int_0^1 \langle \nabla_{\boldsymbol{\eta}} I(\boldsymbol{\eta}(t)), \dot{\boldsymbol{\eta}}(t) \rangle dt, \quad (50)$$

where $\boldsymbol{\eta}(t)$ is any smooth path in the parameter space connecting a reference configuration $\boldsymbol{\eta}_0 = \boldsymbol{\eta}(0)$ to the target configuration $\boldsymbol{\eta}_1 = \boldsymbol{\eta}(1)$. In many practical scenarios, we can choose a reference $\boldsymbol{\eta}_0$ where the mutual information is known

Algorithm 1 Information Gradient Estimation via VJP

Require: DAG \mathcal{G} , target parameter η_k , learned score models s_{ϕ}, s_{ψ} , mini-batch of inputs $\{\mathbf{x}^{(i)}\}_{i=1}^B$.

Ensure: Gradient estimate $\widehat{\nabla}_{\eta_k} I$.

- 1: // 1. **Forward Pass**
- 2: **for** $i = 1$ to B **do**
- 3: Run forward sampling on the DAG from input $\mathbf{x}^{(i)}$ to obtain output $\mathbf{y}^{(i)}$ and all intermediate node values.
- 4: **end for**
- 5: // 2. **Score Difference Calculation**
- 6: **for** $i = 1$ to B **do**
- 7: Compute marginal score: $s_{\text{marg}}^{(i)} \leftarrow s_{\phi}(\mathbf{y}^{(i)})$
- 8: Compute conditional score: $s_{\text{cond}}^{(i)} \leftarrow s_{\psi}(\mathbf{y}^{(i)}|\mathbf{x}^{(i)})$
- 9: Compute score difference vector: $\mathbf{v}^{(i)} \leftarrow s_{\text{cond}}^{(i)} - s_{\text{marg}}^{(i)}$
- 10: **end for**
- 11: // 3. **Backward Pass (VJP)**
- 12: Define scalar VJP loss: $\mathcal{L} \leftarrow -\frac{1}{B} \sum_{i=1}^B \langle \text{stop}(\mathbf{v}^{(i)}), \mathbf{y}^{(i)} \rangle$
- 13: Run backpropagation from \mathcal{L} through the DAG.
- 14: Extract gradient for target parameter: $\widehat{\nabla}_{\eta_k} I \leftarrow -\nabla_{\eta_k} \mathcal{L}$

to be zero (e.g., by setting parameters to zero such that the signal is completely blocked). By numerically integrating the gradient estimates obtained via Algorithm 1 along such a path (e.g., using the trapezoidal rule), we can estimate the absolute value of the end-to-end mutual information for any general DAG.

2) *Fisher Integral Representation*: The mutual information $I(X; Y)$ can be directly estimated by utilizing the connection between differential entropy and Fisher information, known as de Bruijn's identity. Let $Y_0 \equiv Y$ be the DAG output, and consider a noise-corrupted version $Y_t = Y_0 + \sqrt{t}Z'$, where $Z' \sim \mathcal{N}(0, I)$ is an independent standard Gaussian noise vector and $t \geq 0$ is the added noise variance. Recall that the mutual information is the difference of differential entropies: $I(X; Y_t) = h(Y_t) - h(Y_t|X)$. De Bruijn's identity states that the derivative of differential entropy with respect to the noise variance t is proportional to the Fisher information:

$$\frac{d}{dt} h(Y_t) = \frac{1}{2} J(Y_t), \quad \frac{d}{dt} h(Y_t|X) = \frac{1}{2} J(Y_t|X), \quad (51)$$

where $J(Y_t) \equiv \mathbb{E}[\|\nabla_{\mathbf{y}_t} \log p(Y_t)\|^2]$ and $J(Y_t|X) \equiv \mathbb{E}[\|\nabla_{\mathbf{y}_t} \log p(Y_t|X)\|^2]$ are the unconditional and conditional Fisher information, respectively. Consequently, the derivative of mutual information is given by:

$$\frac{d}{dt} I(X; Y_t) = \frac{1}{2} (J(Y_t) - J(Y_t|X)). \quad (52)$$

Using the property that the conditional expectation of the conditional score is the marginal score, i.e., $\mathbb{E}[s_{Y_t|X}(Y_t|X)|Y_t] = s_{Y_t}(Y_t)$, we have the identity

$$J(Y_t|X) - J(Y_t) = \mathbb{E} [\|s_{Y_t|X}(Y_t|X) - s_{Y_t}(Y_t)\|^2]. \quad (53)$$

Substituting this into (52) and integrating from $t = 0$ to ∞ (noting that $\lim_{t \rightarrow \infty} I(X; Y_t) = 0$), we obtain the following integral representation:

$$I(X; Y) = \frac{1}{2} \int_0^\infty [J(Y_t|X) - J(Y_t)] dt \quad (54)$$

$$= \frac{1}{2} \int_0^\infty \mathbb{E} [\|s_{Y_t|X}(Y_t|X) - s_{Y_t}(Y_t)\|^2] dt. \quad (55)$$

This formula allows for estimating $I(X; Y)$ by training score models for varying noise levels t and performing numerical integration. Notably, this approach does not require a reference parameter configuration η_0 with known mutual information, as required in the path-integral method. This integral representation is fundamentally grounded in the score-to-Fisher bridge (SFB) framework introduced in [9].

F. Relation to prior work

A large body of conventional MI estimation and representation learning relies on variational or contrastive bounds (e.g., InfoNCE, CLUB, MINE), which optimize a discriminator or density-ratio model and thus inherit bias-variance and tuning issues from critic training. Non-parametric methods based on kernel density estimation (KDE) [7] or k -nearest neighbors (k NN) [8] are also widely used for MI estimation. However, they often suffer from the curse of dimensionality and are not naturally suited for gradient-based optimization, as differentiating through these estimators with respect to system parameters is computationally prohibitive.

In contrast, our approach does not use a variational lower bound; it expresses the *exact* information gradient as a product of a score difference and a VJP, making it directly amenable to automatic differentiation and avoiding adversarial/contrastive objectives. Classical identities (I-MMSE [17], de Bruijn's identity [14]) relate derivatives of $I(X; Y)$ to MMSE or Fisher information in additive Gaussian settings; we build on these insights but extend them to general nonlinear DAGs and arbitrary internal parameters via a unified gradient formula computable with VJPs. When closed-form scores are unavailable, we leverage DSM (and conditional/posterior variants) to learn the required scores, in contrast to likelihood-ratio or critic-based estimators. For estimating MI values (not only gradients), our path-integral and Fisher-integral representations provide an alternative to density-ratio and variational estimators, enabling integration of readily estimated gradients/Fisher terms.

V. MUTUAL INFORMATION MAXIMIZATION UNDER GLOBAL CONSTRAINTS

The derived information gradient enables the optimization of DAG networks under various practical constraints. In many engineering scenarios, such as power-limited sensor networks or bandwidth-constrained communication systems, the network must be optimized under a global resource constraint rather than individual local constraints.

A. Problem Formulation

We consider the problem of maximizing the end-to-end mutual information subject to a global constraint on the network parameters η . Let $C(\eta) : \mathbb{R}^{\dim(\eta)} \rightarrow \mathbb{R}$ be a differentiable convex cost function representing the total resource usage of the network (e.g., total power consumption defined by an L_2 norm $C(\eta) = \|\eta\|_2^2$). The optimization problem is formulated as

$$\text{maximize}_\eta I(X; Y) \text{ subject to } C(\eta) \leq P, \quad (56)$$

where $P > 0$ is the maximum allowable resource budget.

B. Projected Gradient Ascent

To solve (56), we can employ the *projected gradient ascent* (PGA) method. The PGA algorithm is a standard iterative optimization algorithm suitable for constrained problems where the projection onto the feasible set $\mathcal{S} = \{\eta \mid C(\eta) \leq P\}$ is computationally tractable.

The update rule at iteration t consists of two steps: a gradient ascent step using the estimated information gradient, followed by a projection step onto \mathcal{S} :

$$\tilde{\eta}^{(t+1)} \leftarrow \eta^{(t)} + \alpha_t \widehat{\nabla_\eta I}(\eta^{(t)}) \quad (57)$$

$$\eta^{(t+1)} \leftarrow \mathcal{P}_{\mathcal{S}}(\tilde{\eta}^{(t+1)}). \quad (58)$$

Here, $\alpha_t > 0$ is the learning rate (step size), and $\widehat{\nabla_\eta I}$ is the gradient estimated using Algorithm 1 on a mini-batch of data. The operator $\mathcal{P}_{\mathcal{S}}(\cdot)$ denotes the Euclidean projection onto the feasible set \mathcal{S} :

$$\mathcal{P}_{\mathcal{S}}(\mathbf{v}) \triangleq \arg \min_{\eta' \in \mathcal{S}} \|\eta' - \mathbf{v}\|_2. \quad (59)$$

For common constraints like the global power constraint ($C(\eta) = \|\eta\|_2^2 \leq P$), this projection has a simple closed-form solution (scaling the vector if its norm exceeds \sqrt{P}). By repeating these steps, the network parameters η are updated to maximize the end-to-end information flow while strictly satisfying the global resource constraint.

Remark 6 (Convergence and Non-convexity). In general, the mutual information objective $I(X; Y)$ is non-convex with respect to the network parameters η , particularly when the DAG involves complex nonlinear mappings such as deep neural networks. Consequently, standard gradient-based optimization methods, including the proposed PGA algorithm, are guaranteed to converge only to a stationary point (local optimum or saddle point) of the objective function, not necessarily to the global maximum. Despite this theoretical limitation, gradient-based maximization of MI has been shown to be highly effective in various practical applications.

Remark 7 (Mitigation Strategies for Non-Convexity). To mitigate the risk of getting trapped in poor local optima, several standard practical strategies can be employed. One effective approach is *multi-round optimization*, where the gradient ascent is executed multiple times with different random initializations of η , and the solution with the highest estimated

mutual information is selected. Another promising approach is *noise annealing*. By artificially injecting extra Gaussian noise into Y and gradually decreasing its variance to zero during optimization, the objective landscape is initially smoothed, potentially allowing the optimizer to escape shallow local optima before converging to a final solution.

C. Practical Consideration: Score Drift

A critical challenge in the implementation of PGA algorithm presented above is that updating the network parameters η inherently changes the underlying data distributions $p_Y(\mathbf{y}; \eta)$ and $p_{Y|X}(\mathbf{y}|\mathbf{x}; \eta)$. Consequently, the true score functions “drift” during the optimization process. Using a stale score model trained on an old parameter configuration to estimate gradients for a new configuration can lead to biased or incorrect update directions.

To mitigate this issue, two main strategies can be employed:

- **Iterative Retraining:** The simplest approach is to alternate between score learning and parameter optimization. After every few gradient ascent steps for η , the score models are fine-tuned using fresh samples generated from the current DAG.
- **Conditional Score Networks:** A more advanced approach is to train *conditional* score models $s_\phi(\mathbf{y}; \eta)$ and $s_\psi(\mathbf{y}|\mathbf{x}; \eta)$ that explicitly take the network parameters η as additional inputs. By pre-training these models over the relevant range of η , we can perform optimization without frequent retraining, significantly accelerating the process.

Both strategies present a trade-off between implementation complexity and computational efficiency. Iterative retraining is straightforward to implement and ensures highly accurate local score estimates, but it can become a computational bottleneck during the optimization phase due to frequent retraining. In contrast, conditional score networks significantly accelerate the online optimization phase by eliminating the need for retraining. However, they require a more complex and potentially data-intensive pre-training phase to ensure the model generalizes well across the relevant parameter space of η .

D. Potential Impact and Applications

The proposed framework, which enables end-to-end information-theoretic optimization of general DAGs under global constraints, has significant potential impacts across various domains involving complex stochastic systems.

1) *Next-Generation Wireless Systems (Semantic Communications):* Unlike traditional communications that aim to maximize mere data transmission rates, next-generation paradigms like *semantic communication* [11] focus on maximizing the successful execution of downstream tasks. Our framework naturally supports this goal by treating the entire communication link as a DAG. Crucially, this allows for the joint optimization of transmitter (encoder) and receiver (decoder). By modeling the encoder η_{TX} , the noisy channel, and the decoder η_{RX} as a single unified DAG, we can simultaneously optimize both η_{TX} and η_{RX} to maximize the task-relevant

mutual information $I(T; Y_{\text{final}})$ at the receiver’s decision point, rather than just maximizing channel capacity. This end-to-end approach is particularly valuable when the channel involves complex, nonlinear distortions that are difficult to handle with classical modular designs.

2) *IoT and Distributed Sensor Networks:* Consider a large-scale sensor network where numerous battery-constrained sensors observe a common physical phenomenon X and transmit processed data to a central hub Y . This system forms a massive DAG with a global power constraint $C(\{\eta_i\}) \leq P_{\text{total}}$. Our framework provides a principled way to determine the optimal operational policy (which sensors should be active, how much they should compress data, and how much power they should allocate for transmission) to maximize the aggregated information $I(X; Y)$ at the center.

3) *Deep Learning and Representation Learning:* Deep neural networks (DNNs) can be viewed as deterministic DAGs (or stochastic ones if techniques like dropout or noisy activations are used). Our method offers a direct way to integrate information-theoretic principles, such as the *Information Bottleneck (IB)* principle [12], into DNN training. By utilizing the derived gradients for the IB objective $\mathcal{L}_{\text{IB}} = I(T; Y) - \beta I(X; Y)$, we can train networks to learn representations Y that are maximally informative about a target task T while being minimally informative about the raw input X , thereby improving generalization and robustness.

VI. RELATION TO NETWORK INFORMATION THEORY

The proposed DAG framework is not merely a tool for arbitrary computational graphs but naturally encompasses many fundamental channel models studied in network information theory [1]. By viewing these classical models through the lens of DAGs, our gradient-based approach provides a unified numerical solver for their end-to-end mutual information, capacity or achievable rate maximization problems, even under complex nonlinear or non-Gaussian assumptions where analytical solutions are intractable.

A. Multi-User Channel Models as DAGs

Many canonical multi-user channels can be directly mapped to specific DAG topologies:

- **Multiple Access Channel (MAC):** A MAC with two senders X_1, X_2 and one receiver Y is represented by a DAG where two root nodes merge into a single child node.

$$Y = f_{\text{MAC}}(X_1, X_2; \eta) + Z. \quad (60)$$

Maximizing $I(X_1, X_2; Y)$ under individual power constraints on X_1, X_2 yields the sum-capacity point.

- **Broadcast Channel (BC):** A BC with one sender X and two receivers Y_1, Y_2 corresponds to a DAG where a single root node branches into two leaf nodes.

$$Y_1 = f_1(X; \eta_1) + Z_1, \quad Y_2 = f_2(X; \eta_2) + Z_2. \quad (61)$$

The capacity region involves trade-offs between $I(X; Y_1)$ and $I(X; Y_2)$, often managed by optimizing the input distribution p_X or superposition coding parameters η .

These two channel models are illustrated in Figure 3.

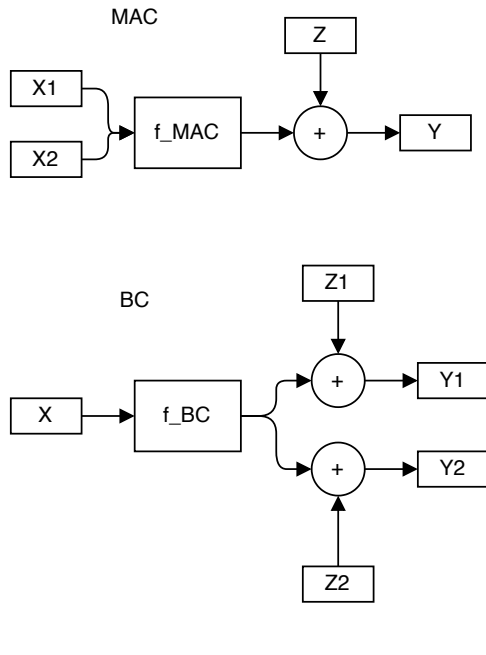


Fig. 3. MAC channel model and BC channel model.

B. A Unified Numerical Solver

Traditionally, finding the capacity regions of these models often requires model-specific analytical techniques (e.g., entropy inequalities, converse proofs), which become extremely difficult when components are nonlinear or non-Gaussian. Our DAG-based information gradient framework offers a *unified numerical approach*: by specifying the graph topology and identifying tunable parameters η (which can parametrize encoders, decoders, or relay functions), one can apply the same generic optimization algorithm (Algorithm 1 + PGA) to numerically discover achievable rate regions for a wide variety of network scenarios.

C. Optimization of Input Distributions

Channel capacity problems often require optimizing the input distribution p_X . Our framework can naturally incorporate this optimization by viewing the input generation process itself as *part of the DAG*. Any distribution that can be sampled from using a computational procedure (e.g., inverse transform sampling, Gaussian mixture models, or deep generative models like VAE, rectified flow [19]) can be represented as a subgraph where the root nodes are primitive noise sources (e.g., multi-dimensional standard Gaussian or uniform random variables). By prepending this generative sub-graph to the main channel DAG, the parameters of the input distribution become standard network parameters η . This enables unified end-to-end gradient-based optimization of both the source distribution

and the channel/system parameters simultaneously, offering a powerful numerical approach for bounding the capacity region of the channel.

D. Unified Procedure for Rate Region Exploration

The information gradient framework developed in this paper provides a unified numerical procedure for exploring rate regions of multi-user channels. For a given parameterization of the input distributions and system components, the resulting rate region defined by mutual information expressions constitutes a bound on the capacity region. When the parameterization is sufficiently expressive to represent the capacity-achieving input distributions, this bound numerically coincides with the true capacity region. We outline the general methodology, which applies to any channel representable as a DAG, regardless of whether analytical solutions exist.

1) *Weighted Sum Maximization*: The boundary of a rate region can be characterized as the Pareto frontier of a multi-objective optimization problem involving multiple mutual information expressions. A standard approach to trace this boundary is to solve a family of weighted optimization problems parameterized by $\lambda = (\lambda_1, \dots, \lambda_K)$ with $\lambda_i \geq 0$:

$$\max_{\theta} \sum_{i=1}^K \lambda_i R_i(\theta) \quad \text{subject to resource constraints,} \quad (62)$$

where $R_i(\theta)$ denotes the i -th mutual information expression, which may be an unconditional mutual information $I(X_i; Y)$ or a conditional mutual information $I(X_i; Y|X_j)$, and θ represents the tunable parameters of the system (e.g., input distribution parameters, encoder weights, or power allocations). By sweeping λ over the probability simplex and solving (62) for each weight configuration, one obtains a collection of boundary points that trace out a bound on the rate region.

2) *Information Gradient for Conditional Mutual Information*: To apply gradient-based optimization to (62), we require the gradient of conditional mutual information with respect to system parameters. Theorem 2 extends naturally to conditional mutual information as follows.

Corollary 3 (Information Gradient for Conditional MI). *For a DAG channel with output Y depending on inputs X_1, X_2 and parameter θ , the gradient of the conditional mutual information $I(X_1; Y|X_2)$ is given by*

$$\begin{aligned} & \nabla_{\theta} I(X_1; Y|X_2) \\ &= \mathbb{E} [(D_{\theta} Y)^{\top} (s_{Y|X_1, X_2}(Y|X_1, X_2) - s_{Y|X_2}(Y|X_2))], \end{aligned} \quad (63)$$

where $s_{Y|X_1, X_2}$ and $s_{Y|X_2}$ are the conditional score functions.

Proof: This follows directly from the decomposition $I(X_1; Y|X_2) = h(Y|X_2) - h(Y|X_1, X_2)$ and applying the same derivation technique as in Theorem 2 to each conditional entropy term. ■

This result, combined with Theorem 2, enables the computation of gradients for all mutual information expressions appearing in standard multi-user channel characterizations,

Algorithm 2 Rate Region Boundary Exploration (Two-User Case)

Require: DAG structure \mathcal{G} , mutual information expressions R_1, R_2 , number of weight samples L , constraint set \mathcal{C}

Ensure: Achievable rate region \mathcal{R}

```

1:  $\mathcal{B} \leftarrow \emptyset$                                  $\triangleright$  Set of boundary points
2: for  $l = 0$  to  $L$  do
3:    $\lambda \leftarrow l/L$                                  $\triangleright$  Weight sweep
4:   Initialize parameters  $\theta$ 
5:   repeat
6:     Generate samples from DAG  $\mathcal{G}$  with current  $\theta$ 
7:     Estimate required score functions via DSM
8:     Compute  $\nabla_\theta R_1$  and  $\nabla_\theta R_2$  using (63)
9:      $\nabla_\theta \mathcal{L} \leftarrow \lambda \nabla_\theta R_1 + (1 - \lambda) \nabla_\theta R_2$ 
10:     $\theta \leftarrow \mathcal{P}_C(\theta + \alpha \nabla_\theta \mathcal{L})$   $\triangleright$  Projected gradient ascent
11:   until convergence
12:   Evaluate  $(R_1^*, R_2^*) \leftarrow (R_1(\theta), R_2(\theta))$  (e.g., via Fisher integral or analytical expressions if available)
13:    $\mathcal{B} \leftarrow \mathcal{B} \cup \{(R_1^*, R_2^*)\}$ 
14: end for
15:  $\mathcal{R} \leftarrow \text{ConvexHull}(\mathcal{B})$            $\triangleright$  Time-sharing achievability
return  $\mathcal{R}$ 

```

including MAC sum-rate $I(X_1, X_2; Y)$ and individual rates $I(X_i; Y|X_j)$.

3) *Algorithmic Framework:* For concreteness, we describe the procedure for a two-user channel (e.g., MAC) where the rate region is characterized by two mutual information expressions $R_1(\theta)$ and $R_2(\theta)$. Algorithm 2 outlines the boundary exploration procedure. The algorithm sweeps a scalar weight $\lambda \in [0, 1]$ over a uniform grid, solves the weighted optimization problem $\max_\theta \lambda R_1 + (1 - \lambda) R_2$ for each λ , and finally computes the convex hull of the resulting points to obtain the rate region.

The final convex hull operation reflects the fact that any convex combination of achievable rate pairs is also achievable via time-sharing between the corresponding coding strategies.

A key practical consideration is *score drift*: as θ evolves during optimization, the underlying distributions change, requiring the score models to be updated. This can be addressed either by periodic retraining of the score networks or by employing conditional score models $s_\phi(y; \theta)$ that take the system parameters as additional inputs, as discussed in Section V-C.

4) *Scope and Future Directions:* The framework presented here establishes the theoretical and algorithmic foundations for rate region exploration via information gradients. While the linear Gaussian case admits analytical verification (see Section VI-E), the primary value of this approach lies in its applicability to channels where closed-form solutions are unavailable, such as nonlinear MACs with $Y = f(X_1, X_2) + Z$ or channels with non-Gaussian noise. For such channels, Algorithm 2 provides a systematic numerical method to explore bounds on the capacity region. Comprehensive numerical studies for specific nonlinear multi-user channels constitute a promising direction for future research.

E. Analytical Validation: Gaussian MAC

To validate Algorithm 2, we consider the linear Gaussian MAC with a sum power constraint. We derive the rate region via two independent routes and demonstrate their equivalence: Route 1 uses the information gradient formula (Corollary 3) with analytical score functions, while Route 2 uses direct differentiation of the known mutual information expressions. The agreement of the resulting rate regions confirms the correctness of the proposed framework.

1) *Channel Model:* Consider a two-user Gaussian MAC defined by

$$Y = X_1 + X_2 + Z, \quad (64)$$

where $X_1 \sim \mathcal{N}(0, P_1)$ and $X_2 \sim \mathcal{N}(0, P_2)$ are independent Gaussian inputs, $Z \sim \mathcal{N}(0, \sigma^2)$ is independent Gaussian noise, and we impose a sum power constraint $P_1 + P_2 \leq P$. The rate expressions are:

$$R_1(P_1) = I(X_1; Y|X_2) = \frac{1}{2} \log \left(1 + \frac{P_1}{\sigma^2} \right), \quad (65)$$

$$R_2(P_2) = I(X_2; Y|X_1) = \frac{1}{2} \log \left(1 + \frac{P_2}{\sigma^2} \right). \quad (66)$$

2) *Route 1: Score-Based Derivation:* We compute the rate region using the information gradient framework. The analytical score functions for this Gaussian channel are:

$$s_{Y|X_1, X_2}(y|x_1, x_2) = -\frac{y - x_1 - x_2}{\sigma^2}, \quad (67)$$

$$s_{Y|X_2}(y|x_2) = -\frac{y - x_2}{P_1 + \sigma^2}. \quad (68)$$

Using the parameterization $X_1 = \sqrt{P_1} \tilde{X}_1$ with $\tilde{X}_1 \sim \mathcal{N}(0, 1)$, we have $D_{P_1} Y = X_1/(2P_1)$. Applying Corollary 3:

$$\nabla_{P_1} R_1 = \mathbb{E} \left[\frac{X_1}{2P_1} (s_{Y|X_1, X_2} - s_{Y|X_2}) \right] = \frac{1}{2(P_1 + \sigma^2)}. \quad (69)$$

By symmetry, $\nabla_{P_2} R_2 = 1/(2(P_2 + \sigma^2))$.

For the weighted objective $\mathcal{L} = \lambda R_1 + (1 - \lambda) R_2$ subject to $P_1 + P_2 = P$, the KKT stationarity conditions using these gradients are:

$$\frac{\lambda}{2(P_1 + \sigma^2)} = \mu, \quad \frac{1 - \lambda}{2(P_2 + \sigma^2)} = \mu. \quad (70)$$

Eliminating μ and solving with $P_1 + P_2 = P$:

$$P_1^{(1)}(\lambda) = \lambda(P + 2\sigma^2) - \sigma^2, \quad (71)$$

$$P_2^{(1)}(\lambda) = (1 - \lambda)(P + 2\sigma^2) - \sigma^2. \quad (72)$$

Substituting into the rate expressions, the boundary points are:

$$R_1^{(1)}(\lambda) = \frac{1}{2} \log \left(\frac{\lambda(P + 2\sigma^2)}{\sigma^2} \right), \quad (73)$$

$$R_2^{(1)}(\lambda) = \frac{1}{2} \log \left(\frac{(1 - \lambda)(P + 2\sigma^2)}{\sigma^2} \right). \quad (74)$$

3) *Route 2: Classical Derivation:* We compute the rate region by directly differentiating the known expressions (65)–(66):

$$\nabla_{P_1} R_1 = \frac{1}{2(P_1 + \sigma^2)}, \quad \nabla_{P_2} R_2 = \frac{1}{2(P_2 + \sigma^2)}. \quad (75)$$

The KKT conditions for $\mathcal{L} = \lambda R_1 + (1 - \lambda) R_2$ subject to $P_1 + P_2 = P$ are identical to (70). Solving yields:

$$P_1^{(2)}(\lambda) = \lambda(P + 2\sigma^2) - \sigma^2, \quad (76)$$

$$P_2^{(2)}(\lambda) = (1 - \lambda)(P + 2\sigma^2) - \sigma^2. \quad (77)$$

The corresponding boundary points are:

$$R_1^{(2)}(\lambda) = \frac{1}{2} \log \left(\frac{\lambda(P + 2\sigma^2)}{\sigma^2} \right), \quad (78)$$

$$R_2^{(2)}(\lambda) = \frac{1}{2} \log \left(\frac{(1 - \lambda)(P + 2\sigma^2)}{\sigma^2} \right). \quad (79)$$

4) *Equivalence of Rate Regions:* Comparing (73)–(74) with (78)–(79), we confirm:

$$\left(R_1^{(1)}(\lambda), R_2^{(1)}(\lambda) \right) = \left(R_1^{(2)}(\lambda), R_2^{(2)}(\lambda) \right), \quad \forall \lambda \in [0, 1]. \quad (80)$$

The two routes produce identical rate region boundaries. Including the corner points at $\lambda \in \{0, 1\}$ where $(R_1, R_2) = (0, \frac{1}{2} \log(1 + P/\sigma^2))$ or $(\frac{1}{2} \log(1 + P/\sigma^2), 0)$, and taking the convex hull, both routes yield the same achievable rate region.

5) *Implications:* This analytical validation demonstrates that Algorithm 2, which implements Route 1 computationally, exactly reproduces the known capacity region derived via Route 2. The key insight is that the score-based information gradient (Corollary 3) provides the correct optimization direction, leading to the same optimal power allocation and hence the same rate region. For nonlinear or non-Gaussian channels where Route 2 is unavailable—since closed-form mutual information expressions do not exist—Route 1 with learned score functions provides the only systematic approach to explore rate region boundaries.

VII. NUMERICAL EXPERIMENTS

A. Information Gradient Estimation on Gaussian Multipath DAG

Before moving on to more complex nonlinear and high-dimensional examples, we first provide a numerical sanity check of Theorem 2 on the linear Gaussian multipath DAG introduced in Sec. IV-C. In that subsection, the DAG structure

$$X \rightarrow (V_1, V_2) \rightarrow Y$$

was specified, and the corresponding effective scalar Gaussian channel $Y = G_{\text{eff}}X + Z_{\text{eff}}$ was derived, together with the closed-form expressions of the mutual information $I(X; Y)$ and its gradients with respect to (η_1, η_2) . In particular, the analytic gradients

$$\frac{\partial I}{\partial \eta_1}, \quad \frac{\partial I}{\partial \eta_2}$$

were obtained in (45) and (46), and their equality with the DAG gradient formula in Theorem 2 was verified analytically

using the Gaussian score functions and the Jacobians $D_{\eta_k}Y$. In the present subsection, we complement this analysis by a fully data-driven Monte Carlo study of the same model.

1) *Experimental setup:* We reuse exactly the same linear Gaussian multipath DAG as in Sec. IV-C, including the variance parameters and the definitions of G_{eff} , σ_N^2 , and v_Y . Unless otherwise stated, we adopt the normalized setting

$$\sigma_X^2 = \sigma_1^2 = \sigma_2^2 = \sigma_3^2 = 1, \quad (81)$$

so that the input and all noise branches have unit variance. We consider two one-dimensional sweeps of the parameters:

- For the first sweep, we fix $\eta_2 = \eta_{2,\text{fix}} = 1$ and vary η_1 over $[\eta_{1,\text{min}}, \eta_{1,\text{max}}] = [-2, 2]$ using K_1 equispaced grid points.
- For the second sweep, we fix $\eta_1 = \eta_{1,\text{fix}} = 1$ and vary η_2 over $[\eta_{2,\text{min}}, \eta_{2,\text{max}}] = [-2, 2]$ with K_2 equispaced grid points.

For each grid point (η_1, η_2) we evaluate the gradients $\partial I / \partial \eta_1$ and $\partial I / \partial \eta_2$ in three different ways:

(i) *Analytic gradient:* We directly evaluate the closed-form expressions (45) and (46) derived in Sec. IV-C; these are treated as ground truth.

(ii) *Monte Carlo gradient with analytic scores:* We apply Theorem 2 to the multipath DAG, using the same Gaussian score functions $s_Y(y)$ and $s_{Y|X}(y|x)$ as in Sec. IV-C and computing the Jacobians $D_{\eta_k}Y$ via reverse-mode automatic differentiation (VJP). Concretely, we estimate

$$\frac{\partial I}{\partial \eta_k} \approx \frac{1}{N} \sum_{n=1}^N (D_{\eta_k}Y^{(n)}) (s_{Y|X}(Y^{(n)}|X^{(n)}) - s_Y(Y^{(n)})), \quad (82)$$

where $(X^{(n)}, Y^{(n)})$ are i.i.d. samples generated by the DAG.

(iii) *Monte Carlo gradient with fully learned scores:* We again use Theorem 2, but now replace both the unconditional score $s_Y(y)$ and the conditional score $s_{Y|X}(y|x)$ by neural score estimators $\hat{s}_Y(y)$ and $\hat{s}_{Y|X}(y|x)$ obtained by denoising score matching (DSM). This setup assumes no knowledge of the true densities, validating the method as a black-box estimator.

For the Monte Carlo estimates (ii) and (iii), we use $N = 10^5$ i.i.d. samples $(X^{(n)}, Z_1^{(n)}, Z_2^{(n)}, Z_3^{(n)})$, generate the corresponding $Y^{(n)}$ through the multipath DAG, and evaluate the gradients with a mini-batch size of 8,192.

2) *Score learning details:* For each grid point (η_1, η_2) we learn score models specific to that channel realization. The training data consists of clean samples sampled from the multipath DAG in Sec. IV-C. We employ two separate MLPs: one for the unconditional score $\hat{s}_Y(y)$ and another for the conditional score $\hat{s}_{Y|X}(y|x)$ (which takes the concatenation of y and x as input). Each network has three hidden layers of width 128, SiLU activations, and a linear output layer.

We train \hat{s}_Y and $\hat{s}_{Y|X}$ by denoising score matching at a fixed noise variance $t_{\text{DSM}} = 0.05$. The unconditional score is trained to denoise Y , while the conditional score is trained

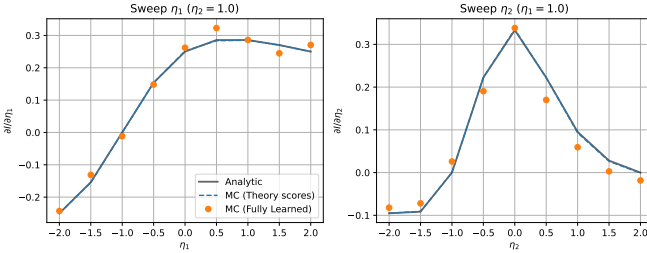


Fig. 4. Information gradients for the linear Gaussian multipath DAG from Sec. IV-C. Left: $\partial I / \partial \eta_1$ as a function of η_1 with η_2 fixed. Right: $\partial I / \partial \eta_2$ as a function of η_2 with η_1 fixed. In each panel, we compare the analytic gradient (solid line), the Monte Carlo evaluation of Theorem 2 with analytic score functions (dashed line), and the Monte Carlo evaluation of Theorem 2 with fully learned scores (markers).

to denoise Y given X . In the reported experiments we use a batch size of 4,096, 500 gradient steps, and the AdamW optimizer with learning rate 10^{-3} .

After training, we apply a scalar Stein calibration to correct global scaling bias of the learned unconditional score \hat{s}_Y . For the one-dimensional output this amounts to the rescaling

$$\tilde{s}_Y(y) = c \hat{s}_Y(y), \quad c = -\frac{1}{\mathbb{E}[Y \hat{s}_Y(Y)]}, \quad (83)$$

which enforces $\mathbb{E}[Y \tilde{s}_Y(Y)] = -1$. In the Monte Carlo gradient (iii), we use \tilde{s}_Y in place of \hat{s}_Y (combined with the raw $\hat{s}_{Y|X}$).

3) *Results:* Figure 4 summarizes the results. The left panel shows $\partial I / \partial \eta_1$ as a function of η_1 with η_2 fixed, while the right panel shows $\partial I / \partial \eta_2$ as a function of η_2 with η_1 fixed. In each panel we plot:

- the analytic gradient (45) or (46) (solid line),
- the Monte Carlo estimate based on Theorem 2 with analytic scores $s_{Y|X}$ and s_Y (dashed line), and
- the Monte Carlo estimate based on Theorem 2 with fully learned scores $\hat{s}_{Y|X}$ and \tilde{s}_Y (markers).

The analytic gradient and the Monte Carlo gradient with analytic scores are indistinguishable at the scale of the plots for both η_1 - and η_2 -sweeps, providing a strong sanity check of the gradient formula in Theorem 2 as well as its VJP-based implementation. Furthermore, the data-driven gradients obtained from the DSM-trained score networks closely track the analytic curves across the entire range of (η_1, η_2) . This demonstrates that the proposed score-learning approach can faithfully reproduce the information gradient even when the DAG is treated as a fully black-box generator of (X, Y) samples, and complements the analytic verification given in Sec. IV-C.

B. Optimization of Multipath DAG under Global Constraint

We apply the proposed information maximization framework to the linear Gaussian multipath DAG defined in Sec. IV-C. The goal is to maximize the end-to-end mutual information $I(X; Y)$ with respect to the parameters $\eta =$

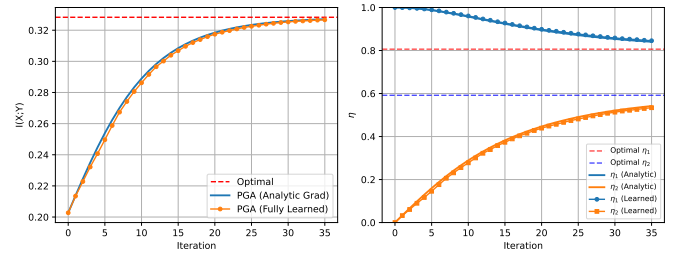


Fig. 5. Maximization of mutual information for the multipath DAG under the constraint $\eta_1^2 + \eta_2^2 = 1$. Left: Evolution of $I(X; Y)$ over PGA iterations. Right: Trajectories of parameters η_1 and η_2 . The proposed fully learned method (markers), which learns both s_Y and $s_{Y|X}$ online with iterative fine-tuning and dual Stein calibration, perfectly tracks the optimal trajectory computed via analytic gradients (solid lines).

(η_1, η_2) subject to a global power constraint $\|\eta\|_2^2 = 1$. This problem serves as a dynamic validation of our framework, assessing whether the gradient estimator remains robust as the underlying data distribution shifts during the optimization process.

1) *Experimental Setup:* We initialize the parameters at $(\eta_1, \eta_2) = (1.0, 0.0)$. We employ the PGA algorithm with a fixed step size of $\alpha = 0.1$ for 35 iterations. At each iteration, we estimate the gradient $\nabla_\eta I(X; Y)$ using Theorem 2. Crucially, to test the fully black-box capability, we assume no knowledge of the analytic score functions. Instead, we estimate the gradient using fully learned scores, where both the unconditional score $s_Y(y)$ and the conditional score $s_{Y|X}(y|x)$ are approximated by neural networks.

2) *Iterative Score Learning Strategy:* Since the distribution of Y (and $Y|X$) changes as η evolves, the score networks must be updated at each PGA step. To handle this efficiently, we adopt a *warm-start* strategy. We maintain two score networks, \hat{s}_Y and $\hat{s}_{Y|X}$, which persist across iterations. At the first iteration ($t = 0$), these networks are trained from scratch for 1,000 steps using DSM to ensure accurate initial gradients. In subsequent iterations ($t > 0$), we update the networks using only 200 steps of DSM, initializing weights from the previous iteration. This fine-tuning approach significantly reduces computational cost while allowing the score models to track the drifting distributions effectively.

Both networks are MLPs with the same architecture as in the previous subsection. For calibration, we apply Stein calibration to both the unconditional and conditional scores at every iteration. Specifically, for the conditional score $\hat{s}_{Y|X}$, we compute a scalar correction factor c satisfying $\mathbb{E}_Y[\mathbb{E}_{Y|X}[(Y - \mathbb{E}[Y|X], c \hat{s}_{Y|X}(Y|X))] = -1$, ensuring robust scale estimates throughout the optimization trajectory.

3) *Results:* Figure 5 presents the optimization results. The left panel shows the trajectory of the mutual information $I(X; Y)$ over iterations, comparing the PGA using the analytic gradient (solid line) and the PGA using the fully learned gradient (markers). The right panel displays the corresponding trajectories of the parameters η_1 and η_2 .

The results demonstrate remarkable agreement between the proposed method and the ground-truth analytic optimization. The fully learned approach steadily maximizes the mutual information, converging to the theoretical optimum (indicated by the red dashed line) at the same rate as the analytic baseline. Furthermore, the right panel confirms that the parameters (η_1, η_2) follow the correct path on the constraint manifold. This experiment confirms that our framework, equipped with the iterative fine-tuning strategy, can successfully drive end-to-end optimization in dynamic settings without access to closed-form likelihoods.

C. Nonlinear scalar channel

Here, we verify that the proposed information-gradient estimator also works reliably for a genuinely nonlinear channel where no closed-form mutual information is available. We consider the scalar model:

$$X \sim \mathcal{N}(0, 1), \quad Z \sim \mathcal{N}(0, \sigma_Z^2), \quad Y = \tanh(\eta X) + Z, \quad (84)$$

with fixed noise variance $\sigma_Z^2 = 0.25$ and scalar parameter $\eta \in [\eta_{\min}, \eta_{\max}] = [-3, 3]$. For each value of η on a small grid, we compute $I(X; Y)$ numerically from the definition $I(X; Y) = h(Y) - h(Z)$. Here $h(Z)$ is analytic, whereas $h(Y)$ is evaluated by first computing $p_Y(y) = \int p_X(x)p_{Y|X}(y|x) dx$ via high-order Gauss–Hermite quadrature over x , and then approximating $H(Y) = -\int p_Y(y) \log p_Y(y) dy$ on a finite interval by a uniform y -grid and the trapezoid rule.

The ground-truth gradient $\partial I / \partial \eta$ is approximated from these values by a centered finite difference

$$\frac{\partial I}{\partial \eta}(\eta) \approx \frac{I(\eta + h) - I(\eta - h)}{2h}, \quad (85)$$

with a small stepsize $h = 0.01$. In parallel, we estimate the information gradient using Theorem 2 with the fully learned scores implementation: both the unconditional score $s_Y(y)$ and the conditional score $s_{Y|X}(y|x)$ are approximated by DSM-trained score networks. Furthermore, both scores are corrected via scalar Stein calibration. The expectation in Theorem 2 is evaluated by Monte Carlo using $N = 10^5$ samples.

Figure 6 summarizes the results.¹ The left panel shows the mutual information $I(X; Y)$ as a function of η , exhibiting the expected even symmetry and saturation as $|\eta|$ increases. The right panel compares the finite-difference gradient and the information gradient obtained from Theorem 2 with fully learned scores. The two curves are nearly indistinguishable over the entire range of η , including around $\eta = 0$ where the true gradient vanishes and in the high-gain regime where $I(X; Y)$ saturates. This experiment indicates that the proposed score-based information-gradient estimator remains accurate and stable even for nonlinear channels where $I(X; Y)$ itself is only available via numerical integration.

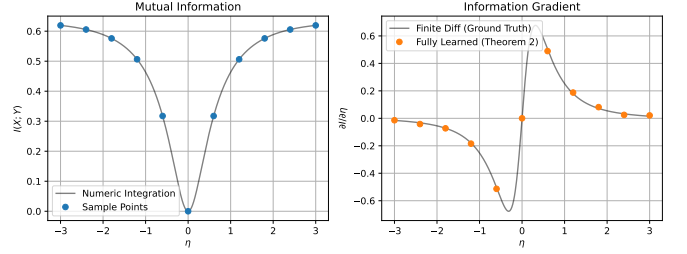


Fig. 6. Nonlinear scalar channel $Y = \tanh(\eta X) + Z$ with $X \sim \mathcal{N}(0, 1)$ and $Z \sim \mathcal{N}(0, 0.25)$. Left: mutual information $I(X; Y)$ as a function of the nonlinearity parameter η , computed by numerical integration of $I(X; Y) = h(Y) - h(Z)$ using Gauss–Hermite quadrature for $p_Y(y)$ and a uniform y -grid. Right: information gradient $\partial I / \partial \eta$ versus η . We compare the finite-difference approximation based on the numerically evaluated $I(\eta)$ (solid line) with the gradient obtained from Theorem 2 using fully learned and Stein-calibrated scores (markers).

VIII. EXTENSION: DIGITAL TWIN CALIBRATION

The information maximization framework presented so far relies on the premise that the DAG model \mathcal{G} accurately represents the real physical system. If there is a significant discrepancy between the model and reality, the parameters η^* optimized in the simulation may fail to perform as expected in the real world. Therefore, calibrating the DAG model to match reality, referred to as *digital twin calibration*, is a prerequisite for practical deployment. In this section, we show that our score-based framework can be naturally extended to address this calibration problem.

A. Problem Formulation

Let the real physical system be governed by an unknown stochastic process that produces output Y_{real} from input X and internal noise sources $\mathcal{Z}_{\text{real}}$:

$$Y_{\text{real}} = g_{\text{real}}(X, \mathcal{Z}_{\text{real}}). \quad (86)$$

Our digital twin is the DAG model defined in (38):

$$Y_{\eta} = g(X, \mathcal{Z}; \eta). \quad (87)$$

We assume that the distributions of inputs X and noise sources \mathcal{Z} in the model match those in the real system. The goal of calibration is to find the parameters η^* that minimize the discrepancy between the real system g_{real} and the DAG model $g(\cdot; \eta^*)$.

B. Score-Based Calibration Strategy

Since the true mechanism g_{real} is unknown and we can only observe samples from Y_{real} , we cannot directly compare the internal functions. Instead, we aim to match their output distributions. Based on the SFB philosophy, we use the Fisher divergence between the real and modeled output distributions as the calibration objective:

$$\begin{aligned} \mathcal{J}_{\text{calib}}(\eta) &\equiv D_F(p_{Y_{\text{real}}} \| p_{Y_{\eta}}) \\ &= \mathbb{E}_{\mathbf{y} \sim p_{Y_{\text{real}}}} [\|s_{Y_{\text{real}}}(\mathbf{y}) - s_{Y_{\eta}}(\mathbf{y}; \eta)\|^2]. \end{aligned} \quad (88)$$

¹See also the numerical curves in the supplementary material.

Minimizing this objective forces the DAG model to generate outputs that are statistically indistinguishable from the real system's outputs (in terms of their score functions). Figure 7 shows the score-based calibration strategy.

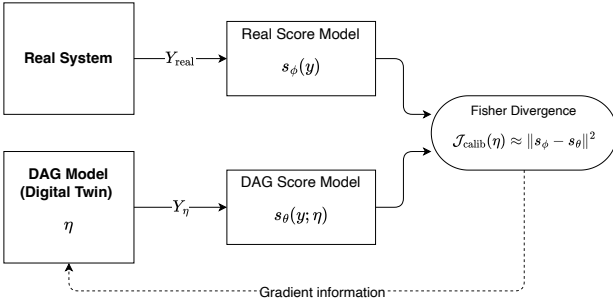


Fig. 7. The score-based calibration strategy. The "Real Score Model" (s_ϕ) is trained on observational data Y_{real} from the physical system. The "DAG Score Model" (s_θ) is trained on simulation data Y_η from the digital twin. The calibration objective $\mathcal{J}_{\text{calib}}(\eta)$ is the Fisher divergence (approximated by the squared difference) between these two score functions. The gradient of this objective is used to update the DAG model parameters η to match reality.

C. Calibration Algorithm via Fisher Divergence Minimization

The optimization of (88) can be performed practically using two types of score models:

- **Real Score Model** $s_\phi(y)$: Learned from observational samples $\{y_{\text{real}}^{(i)}\}$ of the physical system using unsupervised techniques like Sliced Score Matching (SSM), as clean g_{real} is unknown.
- **DAG Score Model** $s_\theta(y; \eta)$: A conditional score network pre-trained on simulation data from the DAG $Y_\eta = g(X, \mathcal{Z}; \eta)$ using standard DSM.

The calibration parameters η are then updated via gradient descent on the estimated Fisher divergence:

$$\eta_{k+1} \leftarrow \eta_k - \alpha \nabla_\eta \mathbb{E}_{y \sim p_{Y_{\text{real}}}} [\|s_\phi(y) - s_\theta(y; \eta_k)\|^2]. \quad (89)$$

This approach allows for calibrating complex, nonlinear DAG models purely from output observations, leveraging the same score-based toolkit developed for information maximization.

Remark 8 (Unsupervised Nature of Calibration). Traditional calibration methods typically require paired input-output data $\{(x^{(i)}, y_{\text{real}}^{(i)})\}$ to minimize element-wise error metrics such as mean squared error (MSE). Gathering such perfectly synchronized paired data from complex physical systems can be operationally difficult or expensive. A distinct advantage of our score-based approach is its *unsupervised* nature; it only requires unmatched observational samples $\{y_{\text{real}}^{(i)}\}$ from the real system (assuming the input distribution p_X is shared). This flexibility significantly broadens the applicability of the framework in real-world scenarios where only output monitoring is feasible.

IX. CONCLUSION

In this paper, we have established a general framework for end-to-end mutual information maximization in complex stochastic systems represented by DAGs. The core contribution is the derivation of the generalized information gradient formula (Theorem 2), which unifies and extends the results in [2] to arbitrary network topologies involving branching, merging, and nonlinear transformations. We demonstrated that this gradient can be efficiently computed by combining modern automatic differentiation tools, specifically VJP, with score matching techniques.

A pivotal advantage of our framework is its capability to operate in a fully black-box manner. As verified in our numerical experiments on both multipath linear DAGs and nonlinear scalar channels, the proposed estimator utilizing neural score models—trained via DSMs and refined by Stein calibration—can faithfully reproduce the true information gradients without requiring knowledge of the underlying likelihood functions. The successful optimization of network parameters under global constraints further confirms the robustness of the proposed iterative score learning strategy against distribution drifts.

Beyond maximization, we showed that the score-based perspective naturally extends to unsupervised model calibration. The proposed digital twin calibration method minimizes the Fisher divergence between a physical system and its model using only output samples, offering a practical solution for aligning simulation environments with reality.

While the accuracy of the gradient estimation naturally depends on the fidelity of the learned score models, the derived theorem itself provides a rigorous and universal interface connecting mutual information to the score function. As score estimation techniques continue to advance, the applicability and precision of this framework will naturally expand.

By bridging the gap between fundamental information-theoretic identities and scalable deep learning computation, this work provides a versatile toolkit for designing next-generation information systems, ranging from semantic communications to distributed sensor networks, where optimizing information flow through complex, unmodeled channels is paramount.

Future work includes applying this framework to rate-distortion analysis and distributed source coding. While this paper primarily focused on maximizing mutual information for channel coding, the proposed information gradient framework is inherently dualistic and applies equally to minimization problems. A promising direction for future work is the application of this framework to rate-distortion analysis and distributed source coding. By interpreting the DAG as a test channel (encoder) and minimizing the mutual information under distortion constraints, our method can serve as a data-driven solver for characterizing the achievable rate regions of complex sensor networks, complementary to the channel capacity problems discussed herein.

ACKNOWLEDGMENTS

This work was supported by JST, CRONOS, Japan Grant Number JPMJCS25N5.

REFERENCES

- [1] T. M. Cover and J. A. Thomas, *Elements of Information Theory*, 2nd ed. Hoboken, NJ, USA: Wiley, 2006. ISBN: 978-0-471-24195-9.
- [2] T. Wadayama, "Information Gradient for Nonlinear Gaussian Channel with Applications to Task-Oriented Communication," <https://arxiv.org/abs/2510.20179>, 2025.
- [3] P. Vincent, "A connection between score matching and denoising autoencoders," *Neural Computation*, vol. 23, no. 7, pp. 1661–1674, Jul. 2011. doi: 10.1162/NECO_a_00142.
- [4] Y. Song and S. Ermon, "Generative modeling by estimating gradients of the data distribution," in *Advances in Neural Information Processing Systems (NeurIPS)*, 2019, pp. 1895–11907. arXiv:1907.05600.
- [5] Y. Song, J. Sohl-Dickstein, D. P. Kingma, A. Kumar, S. Ermon, and B. Poole, "Score-based generative modeling through stochastic differential equations," in *Advances in Neural Information Processing Systems (NeurIPS)*, vol. 34, 2021, pp. 30470–30480. arXiv:2011.13456.
- [6] A. G. Baydin, B. A. Pearlmutter, A. A. Radul, and J. M. Siskind, "Automatic differentiation in machine learning: a survey," *Journal of Machine Learning Research*, vol. 18, pp. 5595–5637, 2018.
- [7] Y.-I. Moon, B. Rajagopalan, and U. Lall, "Estimation of mutual information using kernel density estimators," *Physical Review E*, vol. 52, no. 3, pp. 2318–2321, 1995. doi: 10.1103/PhysRevE.52.2318.
- [8] A. Kraskov, H. Stögbauer, and P. Grassberger, "Estimating mutual information," *Physical Review E*, vol. 69, no. 6, p. 066138, Jun. 2004. doi: 10.1103/PhysRevE.69.066138.
- [9] T. Wadayama, "Mutual information estimation via score-to-Fisher bridge for nonlinear Gaussian noise channels," <https://arxiv.org/abs/2510.05496>, 2025.
- [10] A. Hyvärinen, "Estimation of non-normalized statistical models by score matching," *Journal of Machine Learning Research*, vol. 6, pp. 695–709, 2005.
- [11] D. Gündüz, Z. Qin, Iñaki Estella Aguerri, H. S. Dhillon, Z. Yang, A. Yener, K.-K. Wong, and C.-B. Chae, "Beyond transmitting bits: context, semantics, and task-oriented communications," *IEEE Journal on Selected Areas in Communications*, vol. 41, no. 1, pp. 5–41, Jan. 2023., doi: 10.1109/JSAC.2022.3223408.
- [12] N. Tishby, F. C. Pereira, and W. Bialek, "The information bottleneck method," in *Proc. 37th Annu. Allerton Conf. Commun., Control, and Computing*, Monticello, IL, USA, 1999, pp. 368–377.
- [13] R. A. Fisher, "On the Mathematical Foundations of Theoretical Statistics," *Philosophical Transactions of the Royal Society of London. Series A*, vol. 222, pp. 309–368, 1922. doi: 10.1098/rsta.1922.0009.
- [14] A. J. Stam, "Some inequalities satisfied by the quantities of information of Fisher and Shannon," *Information and Control*, vol. 2, no. 2, pp. 101–112, Jun. 1959. doi: 10.1016/S0019-9958(59)90348-1.
- [15] L. D. Brown, "A proof of the central limit theorem motivated by the Cramér-Rao inequality," *Statistics & Decisions*, vol. 1, pp. 58–68, 1982.
- [16] A. R. Barron, "Entropy and the central limit theorem," *The Annals of Probability*, vol. 14, no. 1, pp. 336–342, Jan. 1986. doi: 10.1214/aop/1176992632.
- [17] D. Guo, S. Shamai (Shitz), and S. Verdú, "Mutual information and minimum mean-square error in Gaussian channels," *IEEE Transactions on Information Theory*, vol. 51, no. 4, pp. 1261–1282, Apr. 2005. doi: 10.1109/TIT.2005.844072.
- [18] Y. Lipman, R. T. Q. Chen, H. Ben-Hamu, M. Nickel, and M. Le, "Flow Matching for Generative Modeling," in *Proc. Int. Conf. Learn. Representations (ICLR)*, 2023. [Online]. Available: arXiv:2210.02747.
- [19] X. Liu, C. Gong, and Q. Liu, "Flow Straight and Fast: Learning to Generate and Transfer Data with Rectified Flow," in *Proc. Int. Conf. Learn. Representations (ICLR)*, 2023. [Online]. Available: arXiv:2209.03003.
- [20] D. P. Kingma and M. Welling, "Auto-encoding variational Bayes," in *Proc. Int. Conf. Learn. Representations (ICLR)*, 2014. [Online]. Available: arXiv:1312.6114.